Supporting Information

Supporting note 1: XRPD pattern and SEM of the A(Lu,Gd)28 glass synthesized through containerless solidification process

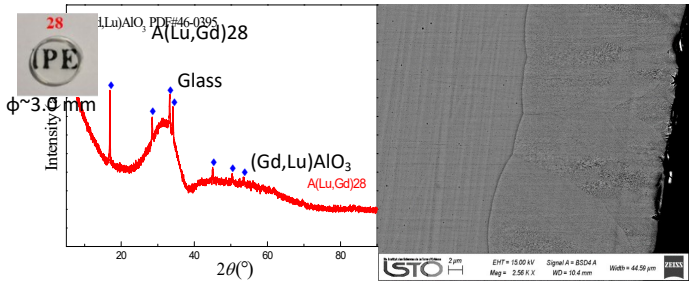

Figure S1. XRPD pattern and SEM of the A(Lu,Gd)28 glass synthesized through containerless solidification process (the thickness of $(Gd,Lu)AlO_3$ is ~10 μm).

Supporting note 2: DSC curve of the A(Lu,Gd)28 glasses (glass beads) synthesized through containerless solidification process

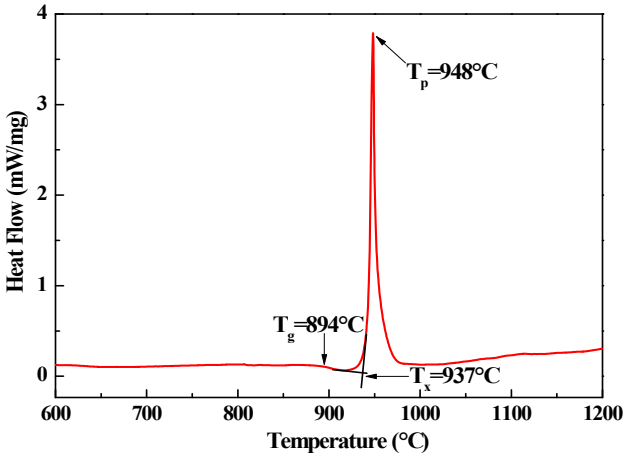

Figure S2. DSC curve of the A(Lu,Gd)28 glasses (glass beads) synthesized through containerless solidification process.

Supporting note 3: SEM backscattering images of transparent ceramics crystallized from A(Lu,Gd)28 bulk glasses

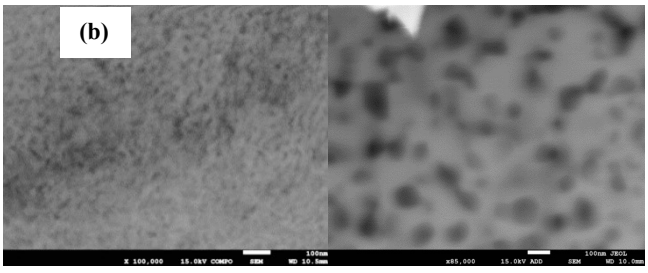

Figure S3. SEM backscattering images of transparent ceramics crystallized from A(Lu,Gd)28 bulk glasses at (a) 1100 °C and (b) 1300 °C.

Supporting note 4: HR-XRPD pattern of transparent ceramics crystallized from A(Lu,Gd)28 glass-based precursors with 20% Gd^{3+} at 1000 °C and 1100 °C

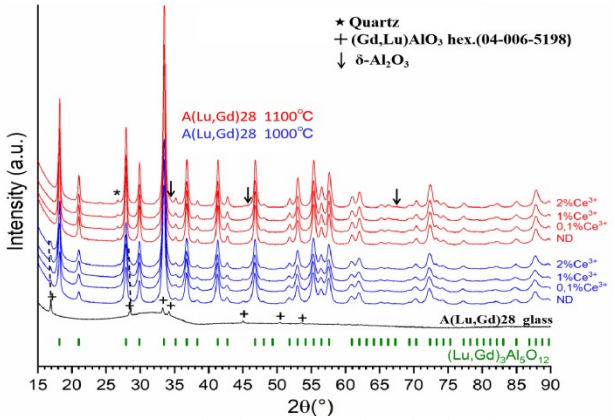

Figure S4. HR-XRPD pattern of transparent ceramics crystallized from A(Lu,Gd)28 glass-based precursors with 20% Gd^{3+} at 1000 °C and 1100 °C for 2 h.

Supporting note 5: Absorption spectrum of Ce:LuGAG-Al_2O_3 transparent nanoceramics with different Ce^{3+} contents

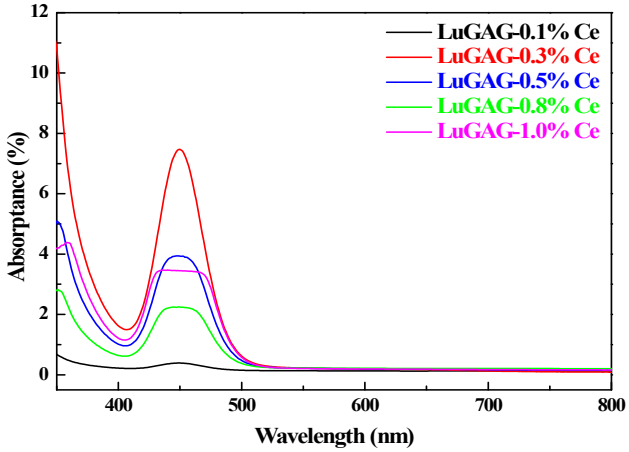

Figure S5. Absorption spectrum of Ce:LuGAG-Al_2O_3 transparent nanoceramics with different Ce^{3+} contents.

Supporting note 6: Variable temperature PL intensity and quantum efficiency of 0.3%Ce:LuGAG-Al_2O_3 transparent nanoceramics

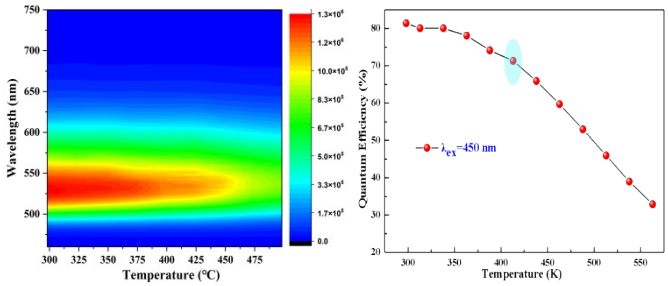

Figure S6. Variable temperature PL intensity and quantum efficiency of 0.3%Ce:LuGAG-Al_2O_3 transparent nanoceramics.